Effects of particle contamination and substrate interaction on the Raman response of unintentionally doped graphene

J. M. Caridad,[1,2,a)] F. Rossella,[1] V. Bellani,[1,b)] M. Maicas,[3] M. Patrini,[1] and E. Díez[2]
[1]*Dipartimento di Fisica "A.Volta" and CNISM, Università degli Studi di Pavia, 27100 Pavia, Italy*
[2]*Laboratorio de Bajas Temperaturas, Universidad de Salamanca, 37008 Salamanca, Spain*
[3]*Instituto de Sistemas Optoelectrónicos y Microtecnología, Universidad Politécnica de Madrid, 28040 Madrid, Spain*

(Received 2 June 2010; accepted 10 September 2010; published online 28 October 2010)

We investigated the inhomogeneities in the charge density of unintentionally doped graphene on SiO_2 prepared by mechanical exfoliation. From the analysis of the G, D, and 2D phonon modes of the Raman spectra after displacing contaminants on graphene surface, and measuring the separation monolayer-substrate distance among zones with different doping levels, we deduce that the interaction with the substrate is the main cause of doping in graphene rather than particle contamination. In particular, we show how graphene doping levels vary within the same flake depending on the distance between graphene and the substrate. © *2010 American Institute of Physics*. [doi:10.1063/1.3500295]

I. INTRODUCTION

Graphene, a single atomic plane of graphite, is the thinnest existing material and offers many unexplored scientific and technological opportunities due to its unique electronic, optical and phonon properties.[1–3] Several methods have been developed to produce graphene. Flakes can be prepared by chemical vapor deposition, carbon segregation from SiC,[4] solubilizing macroscopic quantities of graphene in suspension,[5] or by mechanical exfoliation, which is the most common procedure.[3] Graphene characterization is a key step prior to its processing into nanodevices. At this stage, valuable information about the quality of layers, doping distribution or strain can be obtained using different techniques such as scanning probe microscopy, optical contrast, and light scattering spectroscopy.[6–12] In particular, doping plays a major role in graphene physics as it considerably modifies the transport properties of microdevice and nanodevice based on this material. Recent works have elucidated the underlying processes responsible for doping.[13–15] Scanning tunneling microscopy (STM) studies show that fluctuations of the charged density on the length scale of 20 nm are caused by charge-donating impurities rather than topographical corrugations in the graphene sheet.[16] Electrostatic force microscopy studies reveal that graphene on SiO_2 is effectively doped by a dipole formed at the monolayer–substrate interface.[17] Raman spectroscopy investigations of supported graphene have proved that even unprocessed graphene samples are unintentionally doped.[18–23] In addition, Raman studies comparing pristine free-standing and supported graphene show that its doping is mainly induced by the interaction of graphene with the underlying substrate rather than with atmospheric particles.[24,25] However, the different values of doping levels in supported regions of graphene samples,[24,25] and the observed micro scale fluctuations in the charge density within the same graphene flake,[26] indicate that the actual role of the air contaminants and SiO_2-layer interaction in graphene doping still have to be fully understood. In this work, we present results of an investigation of the inhomogeneous doping levels existent in exfoliated graphene on SiO_2 substrate. This is achieved by preparing graphene monolayers with the mechanical exfoliation technique.[3] Graphene samples are characterized by spatially resolved Raman spectroscopy and atomic force microscopy (AFM). Usually, annealing procedures are used to improve the quality of graphene flakes and devices i.e., to remove atmospheric particle contamination which can dope the sample and consequently shift the charge neutrality point far from 0 V. Indeed, electrical annealing in vacuum, forming gas treatments and thermal annealing (heating the sample above 373 K pumping in vacuum) are very effective at reducing or almost eliminating extrinsic doping ($<5\times10^{11}$ cm^{-2}). Besides, a graphene sample cleaned in vacuum will very rapidly acquire considerable doping (often more than 10^{12} cm^{-2}) once exposed to air. However, we do not consider the effect of previous annealing in our work but we study the correlation between the physical separation among graphene sheets and the amount of extrinsic doping inferred from Raman measurements, having the doping situation typical for a potential graphene device which is likely to work under ambient conditions. Thus, we did not anneal our samples, and we measured it in ambient conditions. Whereas Raman imaging is able to reveal doping levels within the sample,[23,25,27] AFM provides information about the distance d between graphene and SiO_2 substrate. AFM is also used in this work to move existing contaminants on graphene surface. We verify that particle contamination do not significantly dope supported graphene as discussed in Ref. 25. Moreover, we clearly show that the SiO_2-monolayer interaction plays a major role in graphene doping and demonstrate how the charge density levels of graphene vary locally (i.e., within the same flake) depending on the distance between

[a)]Present address: School of Physics, Trinity College Dublin, Dublin 2, Ireland.
[b)]Electronic mail: bellani@unipv.it.

graphene layer and SiO_2. Specifically, analyzing the G, D, and 2D bands, Raman spectra do not reveal important changes before and after moving contaminants with the AFM tip. Thus, with an alternative set-up, we support the findings of Ref. 25, which concludes that the presence of atmospheric particles on the monolayer does not significantly perturb the graphene lattice or cause substantial charge transfer to the graphene layer. Furthermore, by imaging Raman G-band we are able to identify areas with different doping within the same graphene flake, while AFM measurements allow us to obtain the distance d between graphene and substrate for those unequally doped zones. We show how graphene regions with higher d are less doped than areas closer to the substrate. This result confirms that graphene doping strongly depends on the substrate–layer interaction. In addition, we discuss the possible causes of the different d values existent within a flake and comment on the implications of this finding on controlling the doping levels of graphene-based devices.

II. EXPERIMENTAL

For our investigations we utilized Raman spectroscopy and AFM. This allowed us to measure the graphene-substrate distance and the graphene doping levels (without the need for electrodes) and enabled us to displace contaminants existing on the graphene layer. Raman spectroscopy has been proved to be a superb tool for detecting and characterizing graphene and few layer graphite (FLG).[12,18] Raman modes are sensitive to physical parameters such as temperature,[19] strain,[20] defect density,[18,21] and doping levels,[23,27,28] and provide valuable information about the edge structure.[26] Moreover, spatially resolved Raman spectroscopy allows us to measure the variation in these quantities in the mapped region.[24–26] The so-called G, D, and 2D bands are the three main Raman features in carbon allotropes,[12] which lie in graphite around $\sim 1580\ cm^{-1}$, $\sim 1300\ cm^{-1}$, and $\sim 2700\ cm^{-1}$, respectively. The G band corresponds to the E2g phonon at the Brillouin center zone; the D band is due to the breathing modes of sp^2 atoms, and indicates presence of short-range disorder in the graphene flake or armchair chirality at the graphene edges;[18,26] finally, the 2D band is the symmetry-allowed second order of D line and its line shape is commonly used to detect and differentiate graphene from bilayer or FLG.[12] In particular the Raman spectrum exhibits certain variations with doping:[21] the frequency of the G-mode (ω_G) may increase or decrease with doping or charge density (n), depending on the doping type (electron or hole) and level;[27–29] G band line width (Γ_G) decreases for increasing n up to a minimum value;[27,28] the frequency of the 2D mode increases for p-doping while decreases for n-doping with increasing n, and the ratio between 2D line integrated intensity I(2D) and G line integrated intensity I(G), i.e., I(2D)/I(G), decreases for increasing n. Experimental values of ω_G and Γ_G are referred as Pos(G) and FWHM(G) throughout this manuscript and they are calculated as the frequency of the maximum and full-width at half maximum of the G band Lorentzian fit, respectively. Raman spectra were measured at room temperature with a micro-Raman spectrometer (Horiba Jobin-Yvon) with $\sim 1\ cm^{-1}$ spectral resolution, using a $\times 100$ objective (laser spot $\sim 1\ \mu m^2$) and an excitation laser at 632.81 nm wavelength. The multiple spectra measured in each region were treated with a statistical analysis, in order to minimize the error. A notch filter is installed before the charge-coupled device detector to stop the laser light. The calibration was carried out by checking Rayleigh band and Si band at $0\ cm^{-1}$ and $521\ cm^{-1}$, respectively. The graphene regions were scanned with a spatial resolution of $\sim 0.5\ \mu m$ and the acquisition time used for all the positions was of the order of few minutes. Power on the samples was below 1 mW in order to not heat the sample.[19]

AFM is a common tool used to measure the thickness of graphene and FLG.[3,6–8] In this work we used a Digital Instruments MMAFM-2 and a Thermo Microscopes CPII AFM to measure the distance between graphene flake and the substrate at ambient conditions. The measurements in both microscopes were made in tapping mode to not to damage or modify the graphene flakes, using diamondlike carbon coated tips (15 nm nominal radius) and NT-MDT silicon tips (10 nm nominal radius), respectively. We undertook AFM measurements with two different microscopes to rule out any possible dependence of laboratory conditions.[8] Graphene flakes were deposited on Si/SiO_2 substrate by the well-tested method of mechanical exfoliation[3] and the samples were kept for approximately five months under ambient conditions before the Raman and AFM measurement.

III. RESULTS AND DISCUSSION

The monolayers were identified through Raman measurements of the 2D mode and optical microscopy.[12] Explicit formulas for the determination of the doping level (n), $|n| < \sim 2\times 10^{13}\ cm^{-2}$, from the G band line-width [Γ_G or FWHM(G)] and from the G mode frequency [ω_G or Pos(G)] at T=0 K are given in Refs. 22 and 28:

$$\Gamma_G = \frac{\omega_0 \alpha}{4c} \frac{\sinh\left(\frac{-\hbar\omega_0}{2k_BT}\right)}{\cosh\left(\frac{\hbar\omega_0}{2k_BT}\right) + \cosh\left(\frac{E_F}{k_BT}\right)}, \tag{1}$$

$$\omega_G = \omega_0 + \frac{\alpha|E_F|}{\hbar} + \frac{\alpha\hbar\omega_0}{4} \ln\left(\left|\frac{|E_F| - \frac{\hbar\omega_0}{2}}{|E_F| + \frac{\hbar\omega_0}{2}}\right|\right), \tag{2}$$

where $\alpha = 4.43\times 10^{-3}$, ω_0 is the position of the G band in absence of any doping, $E_F = \hbar v_F \sqrt{\pi |n|}$ is the Fermi level, T is the temperature, $v_F \approx 10^6$ m/s is the Fermi velocity, k_B is the Boltzmann constant, $\hbar$ is the reduced Planck constant, and c the speed of the light. For our studies, we found that Pos(G) is a sensitive feature for determining the doping densities of the order of $|n| < \sim 10^{13}\ cm^{-2} (|E_F| \neq \hbar\omega_0/2,)$ since the mode frequency is weakly temperature dependent and Eq. (2) (where T=0 K) can be used[22,28] (see Ref. 30).

Indeed, in accord with Ref. 28, the G mode frequency will increase at increasing electron doping from zero up to

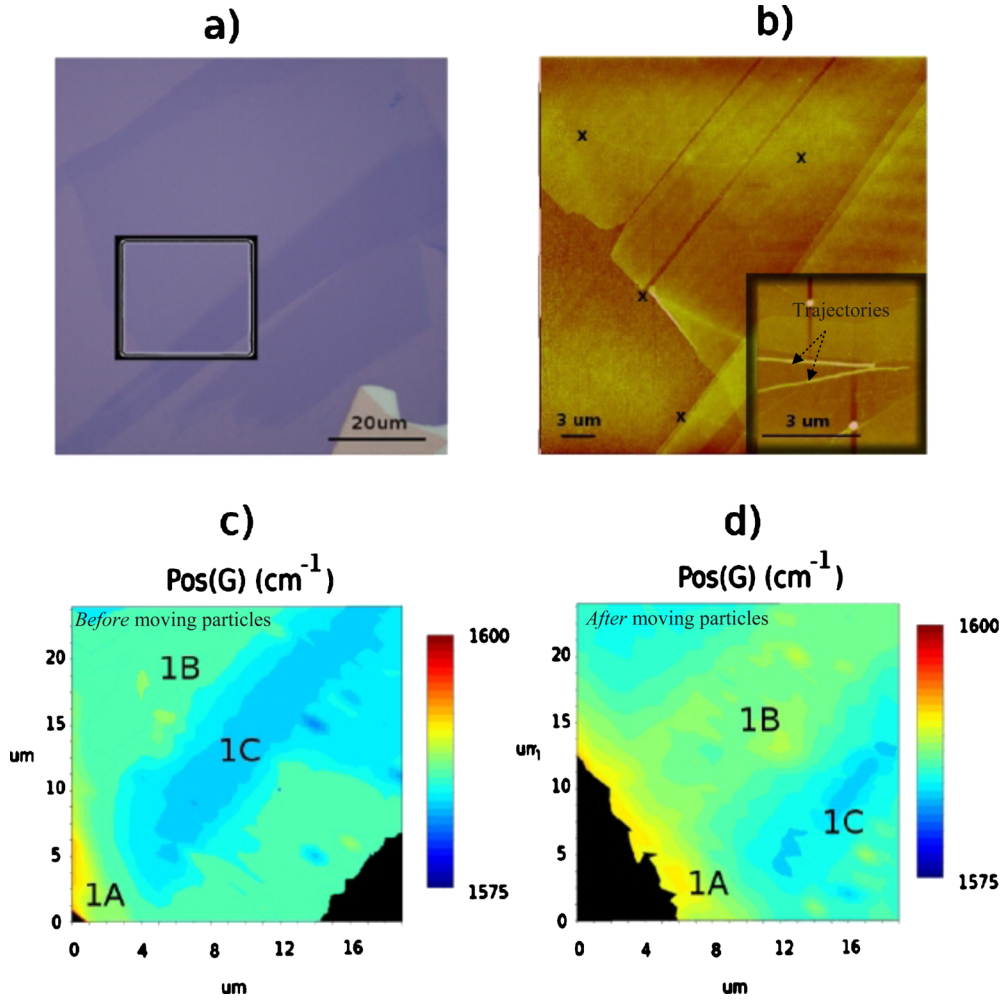

FIG. 1. (Color online) (a) Optical microscope image of graphene and three layer graphite (bottom-right). The manipulation and displacement of contaminants is evidenced by (b) AFM imaging (some starting and ending points of trajectories are marked with *x*; the inset shows the displacement of two contaminants zoomed in) and by the changes induced in Pos(G) imaging of thee area before (c) and after (d) moving the particles.

$\sim 3 \times 10^{13}$ cm^{-2}, which is the typical value for the maximum (intentional) electron doping reachable in a graphene field effect transistor based experiment (although in Ref. 27 it is reported the observation of doping level up to 5 $\times 10^{13}$ cm^{-2} in electrochemically top-gated graphene transistor). We assume to be within this doping regime and we use Eqs. (1) and (2) just as reliable tools to provide an estimation of the doping level from the Raman measurement. In this frame, we consistently observe Pos(G) shifts <8 cm^{-2}. Figure 1(a) shows an optical microscope image of the first sample used in this work. Surface contaminants can be displaced by AFM tip.[31] Indeed, Fig. 1(b) shows displacements of contaminants from left to right in the direction perpendicular to the AFM scanning direction. In particular, the inset in Fig. 1(b) evidences the displacement of two contaminants showing their trajectories. We measured Raman spectra of the area before and after moving the contaminants to observe possible changes in doping levels [Figs. 1(c) and 1(d), respectively]. To quantify this effect, we focus our attention in three main zones (1A, 1B, and 1C). Table I contains the values of Pos(G) and doping values [obtained using Eq. (2)] for these areas before and after the displacement of contaminants. While regions on the left (1A) are less doped after the displacement, zones placed in the middle and mainly on the right part of the flake (1B and 1C) present an increment in doping levels. The possibility of inducing structural disorder when dragging the contaminants is excluded due to two reasons: after the displacement, I(D)/I(G) ratio remains low (smaller than 0.1) and zone 1A is less doped than before moving the particles (disorder induces higher doping[2]). In consequence, we deduce that ambient contaminants can dope graphene lightly ($<5 \times 10^{12}$ cm^{-2}). This result is in agreement with the findings reported in Ref. 25, although it is obtained with a different experimental set-up. Therefore, the main source of doping in SiO_2 supported graphene is the substrate–monolayer interaction rather than atmospheric par-

TABLE I. Pos(G) and estimated doping levels *n* in zones 1A, 1B, and 1C of Fig. 1, before and after the displacement of contaminants.

Zone	Pos(G) before (cm^{-1})	*n* before (cm^{-2})	Pos(G) after (cm^{-1})	*n* after (cm^{-2})
1A	$\sim$1591.8	$\sim 1.47 \times 10^{13}$	$\sim$1591	$\sim 1.35 \times 10^{13}$
1B	$\sim$1589.4	$\sim 1.1 \times 10^{13}$	$\sim$1590.2	$\sim 1.25 \times 10^{13}$
1C	$\sim$1583.8	$\sim 7 \times 10^{12}$	$\sim$1585.4	$\sim 8 \times 10^{12}$

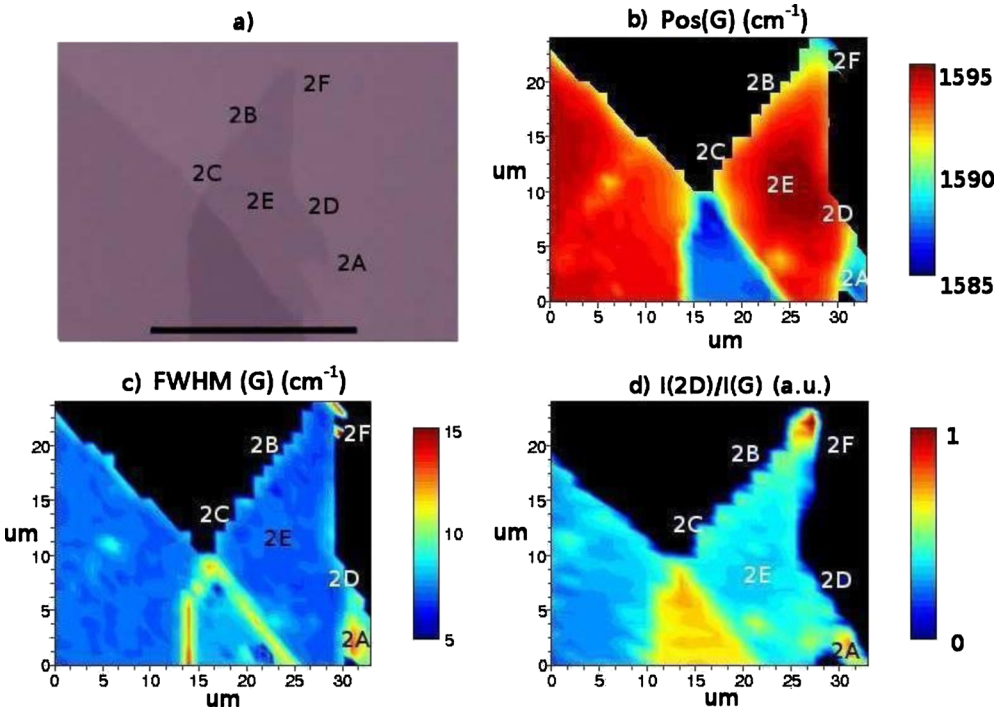

FIG. 2. (Color online) (a) Optical image of grapheme monolayer (right and left) and bilayer (mid bottom). [(b)–(d)] Raman imaging of the flake depending on Pos(G), FWHM(G), and intensity ratio I(2D)/(I(G), respectively. The different doping levels of graphene are shown through variations in these three parameters within the monolayer.

ticles. This outcome does not contradict the STM results obtained by Zhang *et al.*,[16] which show nanometer-sized fluctuations of graphene charge-density (~20 nm) due to impurity doping. As shown before, contaminants do dope graphene slightly, nevertheless, to fully observe the micro size electron/hole puddles in graphene,[26] it is necessary to consider further such responsible effects as the role of layer–substrate interaction. Concerning Raman spectra, measurements on SiO_2 supported graphene samples[25,24] reveal different values of Pos(G) between 1577.6 cm^{-1} and 1594 cm^{-1} (i.e., doping levels between 5×10^{12} cm^{-2} and 2×10^{13} cm^{-2}, respectively). In principle these variations could be due to sample preparation processes. However, doping inhomogeneities on microscale are also appreciable within the same graphene flake,[26] indicating that beyond the sample preparation, graphene-SiO_2 interaction induces doping in the monolayer somehow. To further investigate this interaction, we chose a graphene flake which presented regions with different doping levels [Fig. 2(a)]. The selected regions were free from structural disorder. This is commonly achieved by selecting flake positions without a significant I(D)/I(G) ratio,[22] however, this would exclude border areas with the presence of an armchair edge (D band also appears if armchair chirality is present in the graphene edge).[26] Therefore to distinguish between areas where the D band has originated from disorder and those where it has originated from armchair chirality, we checked if the zones fall in the same FWHM(G)/Pos(G) ratio.[23] This ratio is calculated from Eqs. (1) and (2), eliminating E_F and expressing Γ_G as a function of ω_G (see Ref. 30). From this analysis we derived that 2A–2E are areas without significant disorder, and we excluded structural damaged regions such as 2F. Furthermore, our interpretation of the Raman spectra has neglected the possible influence of strain on the selected sample areas. Given our sample geometry and fabrication method, the existence of isotropic strain can be reasonably excluded. We examined the polarization dependence of the Raman spectra of regions 2A–2E to test the presence of a residual anisotropic strain on Raman G mode. Within our experimental resolution we did not find any shift in the G line of 2A–2E, which rejects any alteration caused by mechanical stress (see Ref. 30). Figure 2(b) shows how Pos(G) substantially varies among the selected zones, thus, exhibiting different doping within the same graphene flake. Mean values of Pos(G), FWHM(G) and an estimation of doping levels of 2A–2E areas through Eq. (2) are reported in Table II. We notice that in our case, less doped areas occur at graphene border. This is a surprisingly result as graphene edges are not as stable, thus bondings with ambient molecules would lead to an increment in doping in these areas, the opposite effect as occurs here. In this case the lower shift in Pos(G) near the edges is accompanied by an increment in FWHM(G) and in

TABLE II. Mean values of Pos(G), FWHM(G), and doping estimation through Eq. (2) for the studied zones within the graphene flake (see Fig. 2).

Zone	Pos(G) (cm^{-1})	FWHM(G) (cm^{-1})	Doping, n (cm^{-2})
2A	1587.6 ± 0.4	10.7 ± 1.0	$\sim9\times10^{12}$
2B	1590.8 ± 0.3	8.4 ± 0.2	$\sim1.35\times10^{13}$
2C	1591.6 ± 0.3	9.0 ± 0.9	$\sim1.6\times10^{13}$
2D	1593.4 ± 0.8	8.5 ± 0.6	$\sim1.7\times10^{13}$
2E	1594.9 ± 0.2	7.3 ± 0.2	$\sim2\times10^{13}$

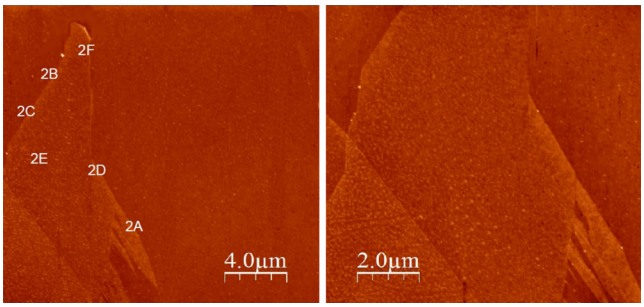

FIG. 3. (Color online) (a) AFM image of the area shown in Fig. 2. (b) Zoom in the regions of interest. It can be noticed that the right edges (2D and 2A) are more raised then the left edge (2C).

the ratio I(2D)/I(G) [Figs. 2(c) and 2(d), respectively]. This evolution of Raman features mimics the behavior reported for suspended graphene,[24,25] and indicates that in these zones the layer is less doped by the substrate. However, it does not mean that graphene borders are always less doped than the flake center; the flake presented in Fig. 1 and other studies show the opposite effect indeed.[26] We exclude that this effect is due to the fact of being close to the edge since the Raman features Pos(G), FWHM(G), and ratio I(2D)/I(G) do not depend on graphene edges[26] but depend on doping.[27,28] These observations suggest that doping in graphene is highly influenced by the interaction with the substrate, however, it is necessary to explicitly prove the relation between graphene doping levels and the distance between graphene and the substrate, *d*. Recent works show that *d* is related not only to the weak interaction between graphene and the SiO_2 surface[9,11,32] but also to chemical bonding or pinnings.[33] These elements corrugate graphene leading to several *d* values within the flake, hence, they could cause different doping

TABLE III. Mean values of *d* for the selected positions A–E.

Zone	*d* (nm)
2A	2.8 ± 0.6
2B	1.4 ± 0.2
2C	1.2 ± 0.2
2D	1.1 ± 0.2
2E	0.7 ± 0.2

levels within the same graphene layer. To confirm this, we performed AFM measurements on the monolayer presented in Fig. 2(a), focusing our attention on the selected zones with different doping values 2A–2E. Figures 3(a) and 3(b) presents the AFM images of the mapped area and shows the different topography of 2A–2E zones. Table III contains the average height values of zones 2A–2E. We note that the height of the corrugations that we observe in our flake agree with the height of ripples recently observed by STM.[34] So far, we have argued the existence of areas within the same graphene flake which posses different doping levels and different distances from the substrate. Figures 4(a)–4(d) shows that these two effects are indeed related. Regions with higher *d* present a shift toward lower values of Pos(G) (a), higher FWHM(G) (b), higher I(2D)/I(G) ratio (c), and lower doping (d). This result clearly connects graphene doping with the graphene-SiO_2 interaction. This finding explains why despite the low effect of atmospheric contaminants on Raman features,[25] measurements of unintentionally doped SiO_2 supported graphene present different values of doping levels [Pos(G)] at micro scale.[24–26] Furthermore, it is in agreement with results obtained in suspended graphene, in which the

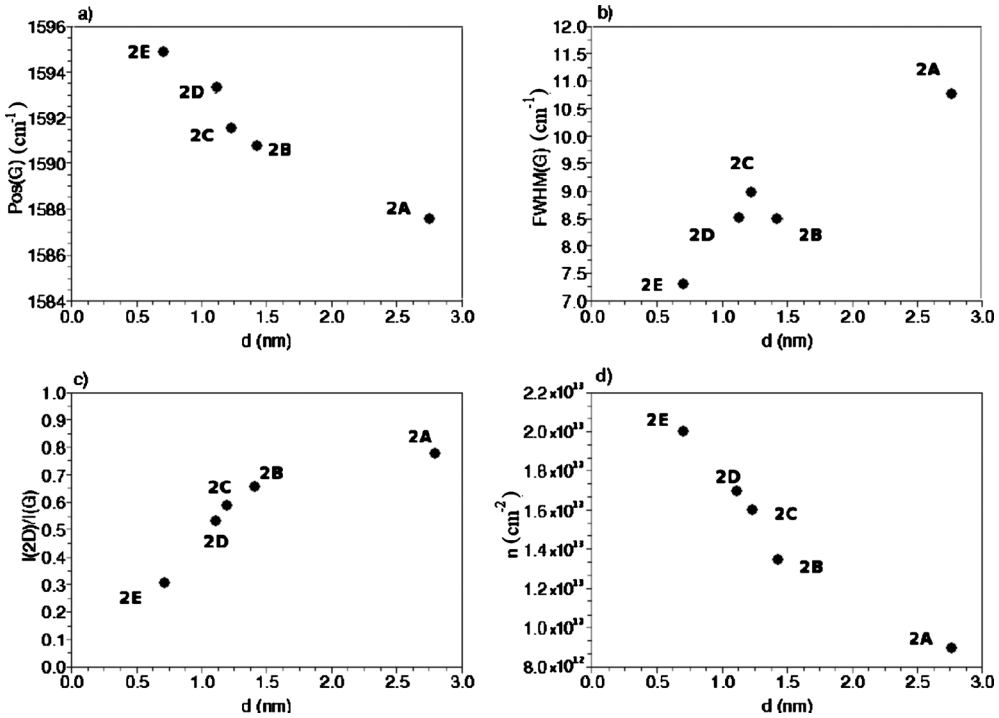

FIG. 4. Raman G peak parameters: (a) position of the peak, Pos(G), (b) its FWHM, (c) I(2D)/I(G) ratio, and (d) the doping level concentration as a function of the distance *d* between graphene and substrate. It can be noticed how graphene zones more raised are less doped and vice-versa.

absence of the interaction with a substrate essentially results in an undoped pristine graphene. This result can be tested with the flake presented in Fig. 1. The average height of zone 1A $(0.6 \pm 0.2$ nm) and its value of Pos(G) $(1593.7 \pm 0.4$ $cm^{-1})$ are in agreement with data showed in Fig. 4 (zones 1B and 1C of the flake are more than 10 μm far from the edge, thus AFM measurements are not reliable due to possible drift). Moreover, we performed AFM and Raman measurements in another flake (flake 3) obtaining identical results (see Ref. 30). Consequently, large variations in charge densities in unintentionally doped graphene on SiO_2 are due to substrate-monolayer interaction, meanwhile ambient contaminants introduce a light doping in the monolayer. These results point toward a promising strategy for precisely controlling the graphene charge density in custom graphene-based nanodevices by tuning d and/or controlling particle contamination in the monolayer.

In conclusion, using Raman scattering and AFM, we have studied the inhomogeneous doped levels which appear in graphene flakes. We focused our study on the influence of two possible causes: atmospheric contaminants on the monolayer and the substrate–graphene interaction. Raman features do not significantly vary when displacing the contaminants placed on top of graphene with the AFM tip, indicating that surface particle contamination do not considerably dope graphene. Instead, we found a clear relation between the graphene–substrate distance and the doping levels in the monolayer. These findings allow us to understand better the nature of the spatial inhomogeneities in the doping level of supported graphene and suggest that the charge transport in graphene may be tailored by engineering the graphene environment.

ACKNOWLEDGMENTS

This work has been financially supported by the Cariplo Foundation (project QUANTDEV) and by the Spanish Ministry of Science and Innovation (Grant Nos. FIS2009-07880, PPT310000-2009-6, and PCT310000-2009-3) and Junta de Castilla y León (Grant No. SA049A10). J.M.C. acknowledges support by the Science Foundation Ireland.

[1] A. H. Castro Neto, F. Guinea, N. M. R. Peres, K. S. Novoselov, and A. K. Geim, Rev. Mod. Phys. **81**, 109 (2009).
[2] A. K. Geim, Science **324**, 1530 (2009).
[3] K. S. Novoselov, A. K. Geim, S. V. Morozov, D. Jiang, Y. Zhang, S. V. Dubonos, I. V. Grigorieva, and A. A. Firsov, Science **306**, 666 (2004).
[4] C. Berger, Z. Song, T. Li, A. Y. Ogbazghi, R. Feng, Z. Dai, N. Alexei, M. E. H. Conrad, P. N. First, and W. A. J. De Heer, J. Phys. Chem. **108**, 9912 (2004).
[5] Y. Hernández, V. Nicolosi, M. Lotya, F. M. Blighe, Z. Sun, S. De, I. T. McGovern, B. Holland, M. Byrne, Y. K. Gunko, J. J. Boland, P. Niraj, G. Duesberg, S. Krishnamurthy, R. Goodhue, R. Hutchison, V. Scardaci, A. C. Ferrari, and J. N. Coleman, Nat. Nanotechnol. **3**, 563 (2008).
[6] A. Gupta, G. Chen, P. Joshi, S. Tadigadapa, and C. Eklund, Nano Lett. **6**, 2667 (2006).
[7] C. Casiraghi, A. Hartschuh, E. Lidorikis, H. Qian, H. Harutyunyan, T. Gokus, K. S. Novoselov, and A. C. Ferrari, Nano Lett. **7**, 2711 (2007).
[8] P. Nemes-Incze, Z. Osváth, K. Kamarás, and L. P. Biró, Carbon **46**, 1435 (2008).
[9] M. Ishigami, J. H. Chen, W. G. Cullen, M. S. Fuhrerand, and E. D. Williams, Nano Lett. **7**, 1643 (2007).
[10] J. C. Meyer, A. K. Geim, M. I. Katsnelson, K. S. Novoselov, T. J. Booth, and S. Roth, Nature (London) **446**, 60 (2007).
[11] U. Stöberl, U. Wurstbauer, W. Wegscheider, D. Weiss, and J. Eroms, Appl. Phys. Lett. **93**, 051906 (2008).
[12] A. C. Ferrari, J. C. Meyer, V. Scardaci, C. Casiraghi, M. Lazzeri, F. Mauri, S. Piscanec, D. Jiang, K. S. Novoselov, and A. K. Geim, Phys. Rev. Lett. **97**, 187401 (2006).
[13] J. H. Chen, C. Jang, S. Adam, M. S. Fuhrer, E. D. Williams, and M. Ishigami, Nat. Phys. **4**, 377 (2008).
[14] J. Martin, N. Akerman, G. Ulbricht, T. Lohmann, J. H. Smet, K. von Klitzing, and A. Yacoby, Nat. Phys. **4**, 144 (2008).
[15] Y. Tan, Y. Zhang, K. Bolotin, Y. Zhao, S. Adam, E. H. Hwang, S. Das Sarma, H. L. Stormer, and P. Kim, Phys. Rev. Lett. **99**, 246803 (2007).
[16] Y. Zhang, V. W. Brar, C. Girit, A. Zettl, and M. F. Crommie, Nat. Phys. **5**, 722 (2009).
[17] Y. Shi, X. Dong, P. Chen, J. Wang, and L. J. Li, Phys. Rev. B **79**, 115402 (2009).
[18] A. C. Ferrari, Solid State Commun. **143**, 47 (2007).
[19] A. C. Calizo, A. A. Baladin, W. Bao, F. Miao, and C. N. Lau, Nano Lett. **7**, 2645 (2007).
[20] M. G. Mohiuddin, A. Lombardo, R. R. Nair, A. Bonetti, G. Savini, R. Jalil, N. Bonini, D. M. Basko, C. Galiotis, N. Marzari, K. S. Novoselov, A. K. Geim, and A. C. Ferrari, Phys. Rev. B **79**, 205433 (2009).
[21] C. Casiraghi, Phys. Status Solidi (RRL) **3**, 175 (2009).
[22] M. Hulman, M. Haluska, G. Scalia, D. Obergfell, and S. Roth, Nano Lett. **8**, 3594 (2008).
[23] C. Casiraghi, S. Pisana, K. S. Novoselov, A. K. Geim, and A. C. Ferrari, Appl. Phys. Lett. **91**, 233108 (2007).
[24] Z. H. Ni, T. Yu, Z. Q. Luo, Y. Y. Wang, L. Liu, C. P. Wong, J. Miao, W. Huang, and Z. X. Shen, ACS Nano **3**, 569 (2009).
[25] S. Berciaud, S. Ryu, L. E. Brus, and T. F. Heinz, Nano Lett. **9**, 346 (2009).
[26] C. Casiraghi, A. Hartschuh, H. Quian, S. Pisanec, C. Georgi, A. Fasoli, K. S. Novoselov, D. M. Basko, and A. C. Ferrari, Nano Lett. **9**, 1433 (2009).
[27] A. Das, S. Pisana, B. Chakraborty, S. Pisanec, S. K. Saha, U. V. Waghmare, K. S. Novoselov, H. R. Krishnamurthy, A. K. Geim, A. C. Ferrari, and A. K. Sood, Nat. Nanotechnol. **3**, 210 (2008).
[28] M. Lazzeri and F. Mauri, Phys. Rev. Lett. **97**, 266407 (2006).
[29] S. Pisana, M. Lazzeri, C. Casiraghi, K. S. Novoselov, A. K. Geim, A. C. Ferrari, and F. Mauri, Nature Mater. **6**, 198 (2007).
[30] See supplementary material at http://dx.doi.org/10.1063/1.3500295 for determination of doping level, disorder, and polarization effects.
[31] T. Junno, K. Deppert, L. Montelius, and L. Samuelson, Appl. Phys. Lett. **66**, 3627 (1995).
[32] T. Li and Z. Zhang, J. Phys. D: Appl. Phys. **43**, 075303 (2010).
[33] J. Sabio, C. Seoánez, S. Fratini, F. Guinea, A. H. Castro Neto, and F. Sols, Phys. Rev. B **77**, 195409 (2008).
[34] K. Xu, P. Cao, and J. R. Heath, Nano Lett. **9**, 4446 (2009).